fMRI measurements of color in macaque and human

Alex Wade Smith-Kettlewell Eye Research Center, San Francisco, CA, USA

Mark Augath Max Planck Institute for Biological Cybernetics, Tübingen, Germany

Nikos Logothetis Max Planck Institute for Biological Cybernetics, Tübingen, Germany

Brian Wandell Psychology Department, Stanford University, Stanford, CA, USA

We have used fMRI to measure responses to chromatic and achromatic contrast in retinotopically defined regions of macaque and human visual cortex. We make four observations. Firstly, the relative amplitudes of responses to color and luminance stimuli in macaque area V1 are similar to those previously observed in human fMRI experiments. Secondly, the dorsal and ventral subdivisions of macaque area V4 respond in a similar way to opponent (L − M)-cone chromatic contrast suggesting that they are part of a single functional area. Thirdly, we find that macaque area V4, like area V1, responds preferentially to chromatic contrast compared to luminance contrast and the degree of preference is strongly influenced by the temporal frequency of the stimulus. Finally, we observe that while macaque V4d is a region on the dorsal surface of the macaque visual cortex that responds robustly to chromatic stimuli, human chromatic responses to identical stimuli are largely confined to the ventral surface suggesting a fundamental difference in the topographical organization of higher visual areas between humans and macaques.

Keywords: color vision, functional imaging, visual cortex, color appearance/constancy

Citation: Wade, A., Augath, M., Logothetis, N., & Wandell, B. (2008). fMRI measurements of color in macaque and human. *Journal of Vision, 8*(10):6, 1–19, http://journalofvision.org/8/10/6/, doi:10.1167/8.10.6.

Introduction

The study of human color vision has generated perhaps the most complete and quantitative description of a perceptual pathway currently available to science. Our understanding of the initial physical and cellular mechanisms of color perception spans a range of disciplines from the sequence, arrangement, and significance of individual opsin genes (Nathans, 1989; Neitz & Jacobs, 1990) through to the development and patterning of the cone photoreceptor mosaic (Roorda & Williams, 1999) and its subtle relationship to physiological optics (Williams & Coletta, 1987; Williams, Sekiguchi, & Brainard, 1993). Color vision truly begins when the three types of cones photoreceptors, with three unique absorption spectra, sample the retinal irradiance across the retina (Baylor, 1987). Retinal circuitry then recombines the cone responses into three relatively independent spatio-chromatic opponent channels (Field & Chichilnisky, 2007; Hurvich & Jameson, 1957; Solomon & Lennie, 2007; Wandell, 1995). The chromatic tuning of these three independent channels can be measured in neurons in the lateral geniculate nucleus (LGN) as they relay the retinal signals to cortex (Derrington, Krauskopf, & Lennie, 1984; De Valois & Jacobs, 1968).

The challenge ahead is to develop a better understanding of the way in color is processed in cortex. The circuitry in primary visual cortex (V1) receives LGN inputs in cortical layers 4Cα, 4Cβ, and 2/3 (Chatterjee & Callaway, 2003) and then transforms the three distinct channels into a diverse set of neural pathways (Johnson, Hawken, & Shapley, 2001, 2004) whose chromatic properties depend upon other stimulus attributes such as size and spatial frequency (Solomon, Peirce, & Lennie, 2004; Solomon, White, & Martin, 2002).

Several lines of evidence suggest that signals communicated to ventral occipital and temporal extrastriate cortex are important to color appearance. In humans, damage to ventral occipital cortex can produce a color-specific deficit, 'achromatopsia' (Bouvier & Engel, 2006; Meadows, 1974; Rüttiger et al., 1999; Zeki, 1990a). Human achromatopes report that their perception of color changes: the world becomes monochromatic or dulled. However, their ability to discriminate objects based solely on their chromaticity is preserved (Cowey, Heywood, & Irving-Bell, 2001; Heywood & Cowey, 1987; Heywood, Wilson, & Cowey, 1987; Kennard, Lawden, Morland, &

Ruddock, 1995; Mollon, Newcombe, Polden, & Ratcliff, 1980). In addition, stimulation of human ventral occipital regions using implanted cortical electrodes generates the sensation of color (Murphey, Yoshor, & Beauchamp, 2008). Finally, ventral human cortical regions respond powerfully to chromatic stimuli in functional MRI (fMRI) experiments (Bartels & Zeki, 2000; Brewer, Liu, Wade, & Wandell, 2005; Hadjikhani, Liu, Dale, Cavanagh, & Tootell, 1998; Takechi et al., 1997; Wade, Brewer, Rieger, & Wandell, 2002; Zeki, 1990b). However, the apparent preference for chromatic stimuli in ventral human occipital cortex is conflated with a bias towards foveal stimuli with low temporal frequency. This bias is not shared by dorsal cortical areas: for example, hMT+ and V3A are more effectively driven (per unit cone contrast) by high-frequency achromatic stimuli (Liu & Wandell, 2005; Mullen, Dumoulin, McMahon, de Zubicaray, & Hess, 2007).

To complete a model of the cortical color circuitry, we need to develop a better understanding of cortical color coding. It is likely that regions homologous to human ventral occipital cortex are present in the macaque monkey, a trichromatic primate whose behavioral performance is quite similar to human (De Valois, Jacobs, & Abramov, 1964). Thus, it should be possible to combine electrophysiological measurements in macaque with human functional imaging to guide the design of computational models. Progress to date has been limited by uncertainty concerning the correspondence between visual field maps in human and macaque. One important source of uncertainty concerns the correspondence between the fourth retinotopic field map in macaque (which we call mV4 in this paper) and the human map (hV4). This relationship is of particular interest because Zeki found that mV4 has a high density of chromatically tuned cells (Essen & Zeki, 1978; Zeki, 1983), and he concluded that this map is essential for color perception (Zeki, 1993; but see Schein, Marrocco, & de Monasterio, 1982; Heywood, Gadotti, & Cowey, 1992). It is clear that lesions in macaque V4 can reduce color discrimination performance and produce abnormal color constancy judgments, along with other visual disturbances (Heywood & Cowey, 1987; Walsh, Carden, Butler, & Kulikowski, 1993; Walsh, Kulikowski, Butler, & Carden, 1992), but there is some uncertainty about whether lesioning macaque V4 is a good model for human achromatopsia, and even which human cortical area mV4 corresponds to.

The uncertainties about the correspondence between mV4 and human maps arise from several sources and they involve questions about visual field map topography and neurological case studies as well as direct functional measurements.

It is generally agreed that the macaque visual field map mV4 is arranged into two parts. One part (mV4d) is located on the dorsal surface adjacent to V2d and V3d. Receptive fields in mV4d are located in the lower visual field. A second part, mV4v, is on the ventral surface, abutting the ventral portion of V3; the receptive fields in this section cover the entire upper visual field but also extend to represent regions below the horizontal midline (Figure 9 of Gattass, Sousa, & Gross, 1988).

In humans a purely ventral lesion damaging hV4 can produce achromatopsia in an entire visual hemifield. However, if we believe that achromatopsia can be caused by damage to area hV4 and if hV4 is the human homologue of mV4v, then a lesion in this 'ventral' hV4 should produce at most a quarterfield achromatopsia. This problem was noted in the important 1974 Meadows paper: "there is still a problem in relating these two areas, for the human evidence is compatible with a colour-coded area close to the striate cortical representation of only the upper part of the vertical meridian of the visual field, whereas in the monkey area V4 appears to extend along the entire vertical meridian. Whether these 2 areas are comparable must therefore await further studies" (pp. 627–628). We expand on this issue in the Discussion.

Direct comparisons of human and macaque visual field maps cannot completely resolve the issue of the mV4/hV4 homology. Our previous work has shown that in humans there is ventral visual field map which we term hV4, representing a hemifield entirely adjacent to V3 ventral (Brewer et al., 2005; Wade et al., 2002). While the location of this map and the adjacent VO-1/2 maps corresponds well with the location of lesions in the 11 pure achromatopes in the literature (Bouvier & Engel, 2006; Wandell, Dumoulin, & Brewer, 2006), the topography of the hV4 field map does not match that of mV4.

To add to the confusion, there is further uncertainty about the integrity of the hV4 map itself. Some investigators suggest that hV4 is still divided into two parts just as its macaque counterpart is, but that the dorsal component is very small and represents a correspondingly restricted set of visual field angles (Hansen, Kay, & Gallant, 2007). In a sense, this would be a species-specific extension of the partial representation of lower visual field found in mV4d (Gattass et al., 1988). This hypothesis is different to our original proposal (Brewer et al., 2005; Wade et al., 2002) and it also modifies a recent scheme for subdividing lateral occipital cortex into two retinotopic regions (LO1 and LO2) proposed by other investigators (Larsson & Heeger, 2006). Also, human measurements identifying cortical regions with strong color selectivity are overwhelmingly ventral and cover a region of cortex that includes hV4 (Bartels & Zeki, 2000; Brewer et al., 2005; Hadjikhani et al., 1998; Howard et al., 1998; Wade et al., 2002; Zeki et al., 1991). However, because the putative hV4d is very small, it is possible that this region has been overlooked in other studies (Wandell, Dumoulin, & Brewer, 2007). We note that the existence of a small lateral V4d would not substantially change the interpretation of our hV4 maps and this region could also coexist with the Larsson and Heeger (2006) LO1/LO2 model. We explicitly address this possibility in our Results section.

A final question concerns the *functional* (as opposed to the topographic) integrity of mV4. Some investigators have speculated that the functional properties of mV4d and mV4v differ, and they ask whether these two cortical zones are truly part of a single functional visual area (Fize et al., 2003). Because it is generally easier to make electrophysiological measurements in mV4d, most macaque data are taken from this dorsal mV4 region and there are very few comparisons of functional responses in dorsal and ventral mV4. The issue of their functional similarity is therefore worth exploring.

The purpose of the experiments reported here is to advance our understanding of the relationship between human and macaque cortical color representations and to compare responses in mV4 and hV4. We make two specific contributions. First, we compare human and macaque functional responses in mV4 and hV4 using similar stimuli and methods. Second, we compare the color responsivity in dorsal and ventral mV4. These data are useful in clarifying the functional similarity of hV4 and mV4 and can be used to evaluate whether mV4d and mV4v are part of a unitary or distinct functional zones (Fize et al., 2003).

Methods

Macaque studies

We measured fMRI data in five anesthetized macaque monkeys in six separate sessions. The fMRI and analysis protocols are described in Logothetis, Guggenberger, Peled, and Pauls (1999). The visual field maps were identified using the methods described by Brewer, Press, Logothetis, and Wandell (2002).

We present surface rendered data for a single monkey for illustrative purposes in Figure 2. Not all monkeys had well-defined retinotopic maps in both hemispheres and so in some cases only a single hemisphere's worth of data could be analyzed. Further, not all animals were run in all chromatic conditions. Figure 3 shows data from seven hemispheres in five monkeys. Figure 4 show data from two hemispheres in a single monkey. Figure 5 shows data from five hemispheres in three monkeys. Retinotopic mapping data from all monkeys are shown in the supplementary material.

MRI parameters

Multislice fMRI was performed by the use of multishot (segmented) gradient-recalled echo-planar imaging (EPI). Volumes of 17 slices were collected, each with a field of view of 128 × 128 mm on a 128 × 128 matrix (1 × 1 mm in-plane resolution) and 2-mm slice thickness. The acquisition parameters were echo time, 20 msec; repetition time, 750 msec; flip angle, 40°; EPI zero phase, 8.192 msec or 40% of phase steps; pulse length, 3.0 msec; spectral width, 100 kHz; line acquisition time, 1.28 msec; number of segments, 8 or 16; segment acquisition time (MRI readout window width), 20.48 msec, repetition time between slices, 37.59 msec; and number of excitations per phase encode step, one. To minimize the effects of inflow and of large drainage vessels, flip angles that were 10–20° smaller than the computed Ernst angle were used. fMRI data were co-registered to anatomical T1-weighted MPRAGE scans acquired on different dates with an isotropic voxel resolution of 0.5 × 0.5 × 0.5 mm.

Animal preparation

Five healthy juvenile monkeys weighing 6–9 kg were used for these experiments. All sessions were performed with great care to ensure the well-being of the monkeys, were approved by the local authorities (Regierungspraesidium), and were in full compliance with the guidelines of the European Community (EUVD 86/609/ EEC) for the care and use of laboratory animals. The monkeys were anesthetized during the experiments. Details on the anesthesia protocol have been given previously. Briefly, the animals were preoxygenated, and anesthesia was induced with fentanyl (31 μg/kg), thiopental (5 mg/kg), and succinylcholine chloride (3 mg/kg). Muscle relaxation was achieved with mivacurium chloride (5 $mg{\cdot}kg^{-1}{\cdot}h^{-1}$). Body temperature was kept constant, and lactated Ringer's solution was given at a rate of 10 $mg{\cdot}kg^{-1}{\cdot}h^{-1}$. Intravascular volume was maintained by administering colloids (hydroxyethyl starch, 30–50 ml over 1–2 min as needed). Monitoring within the magnet was mostly stable and reliable. The depth of anesthesia was assessed continuously by monitoring the vital signs of the monkey and responding accordingly, but because discomfort or stress would be masked by muscle paralysis, we first adjusted the depth of anesthesia before commencing paralysis, and we took the extra precaution of examining the concentration of plasma stress hormones (Logothetis et al., 1999). Anesthesia was always maintained by constant infusion of 0.5–2.0 μg/kg/min of remifentanil that proved to ensure that the stress hormones remained within the normal physiological range.

Optical corrections

Two drops of 1% ophthalmic solution of the anticholinergic cyclopentolate hydrochloride were placed into each eye to achieve cycloplegia and mydriasis. Refractive errors were measured after the induction of paralysis, ~1 hour after the application of cyclopentolate. Contact lenses (Harte PMMA-Linsen Firma Wöhlk, Kiel, Germany) with the appropriate dioptric power were used to bring the animal's eye to a focus onto the stimulus plane (2 diopters).

Visual display system

Visual stimuli were created on a display using a resolution of 1024 × 768 pixels with a 60-Hz frame rate (SilentVision 2000, Avotec Inc, FL). The display image was brought to the animal's eyes within the scanner by a fiber-optic projection system (530 × 400 fibers). The field of view visual angle was a 30° horizontal by 23° vertical; the focus was fixed at 2 diopters. Binocular presentations were accomplished through two independently positioned plastic fiber-optic glasses. A modified fundus camera (RC250; Zeiss, Thornwood, NY) served to position the stimulus, observe the eye fundus, and establish the 30° horizontal × 23° vertical calibration frame. This process ensured the alignment of the stimulus center with the fovea of each eye.

Stimuli

Visual field maps were measured using expanding rings and rotating wedges. These stimuli produce a traveling wave of activity in retinotopically organized visual areas (DeYoe et al., 1996; Engel et al., 1994; Sereno et al., 1995). The stimuli were set to a period of 72 seconds, and each scan included 14 total cycles. The first two were discarded to avoid transient effects, so that the data from each voxel spanned 864 (72 × 12) seconds. At least three and usually four repeats of both the wedge and ring scans were performed on each animal. Retinotopic mapping procedures were similar to those described in Brewer et al. (2002).

Chromatic stimuli were generated using the Psychophysics Toolbox (Brainard, 1997). Cone contrasts were computed using the Stockman cone fundamentals (Stockman, MacLeod, & Johnson, 1993) which have been shown to be essentially identical to those of macaque (Baylor, Nunn, & Schnapf, 1987; Schnapf, Kraft, Nunn, & Baylor, 1988). The display system was calibrated independently for each eye according to the general principles described by Brainard (1989). Radiometric calibration was performed using a fiber-optic photospectrometer (USB2000, OceanOptics FL) and a temporal calibration was performed using a photodiode attached to a digital oscilloscope (TDS420A, Tektronix Inc, Beaverton, OR). Stimuli were presented against a mean-gray background with approximately equal luminance (30 cd·m^{-2}) for each eye.

A typical chromatic stimulus was comprised of a grid of 12 × 12 square patches (Figure 1). Each patch subtended 1° of visual angle and the entire array subtended 12° of visual angle on each side. The color and luminance of the patches were updated at 1 Hz in order to provide temporal as well as spatial contrast. The stimulus color and contrast were specified in cone coordinates. On each update, the chromaticity of each patch was drawn at random from either a single direction in MacLeod–Boynton space or the sum of two such random draws. Hence, each patch contained either a random achromatic contrast, or a random L − M contrast or a sum of both types of contrast.

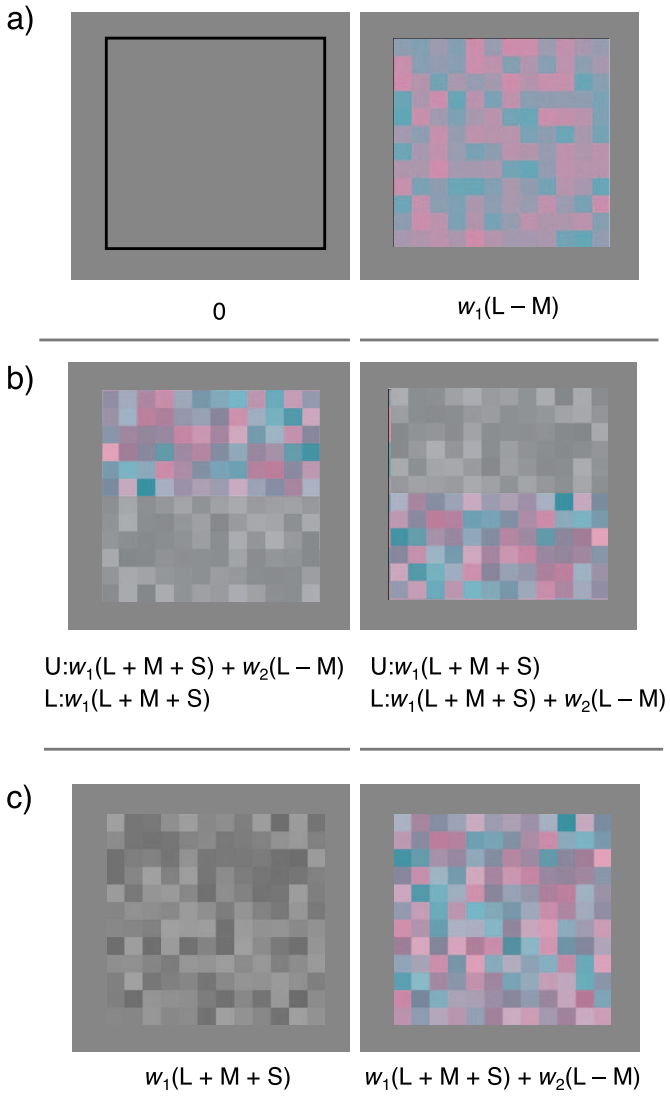

Figure 1. Diagrams of stimuli used in the macaque and human versions of our experiments. (a) Full field alternation of a blank field with textured chromatic or achromatic contrast. (b) Adding contrast in one dimension to constant dynamic contrast in another dimension. Upper versus lower visual field. (c) Adding contrast in one dimension to constant contrast in another dimension. Full field alternation. Arrays subtend 12 degrees of visual angle and contain 12 × 12 square patches. Contrast patterns in the addition experiments (b, c) are updated at 1 Hz with a new random draw from the same color space. The contrast versus blank condition (a) was run at update rates of either 1 or 7 Hz.

The stimulus cone-contrast variations were chosen from one of two axes: L − M (approximately red-green) or L + M + S (achromatic luminance) (MacLeod & Boynton, 1979). We estimated the cone isolation error due to the limited (8-bit) quantization range of the display system. The unwanted stimulus crosstalk between the L − M and L + M + S cone directions was computed to be 1.5% and 4.2%, respectively. In other words, a stimulus with RMS cone contrast of 10% in the L + M + S direction in

MacLeod–Boynton space generated a modulation of no more than 0.42% in the L − M cone direction.

We used a maximum cone contrast of 6% in the L − M (opponent red-green) direction and 24% in the L + M + S (luminance) direction unless otherwise specified. These contrast levels were chosen in order to generate approximate equal responses in area V1 based on the relative sensitivities to these chromatic directions measured using fMRI in humans (Engel, Zhang, & Wandell, 1997). This procedure follows the method used in our human studies (Brewer et al., 2005; Wade et al., 2002).

In the following description, we refer to the constant 'background' contrast direction as C1 and the added or 'probe' contrast direction as C2. Using this design, which is similar to that used by Barbur, Harlow, and Plant (1994), we maintain a constant signal in, say, the luminance direction while varying specific chromatic directions. We used three types of chromatic stimuli.

1. Full-field contrast vs. blank (Figure 1a). In the first type of experiment, we used only a single chromatic direction and we alternated color contrast grids with a blank, gray screen (24-second periods). This experiment was similar to those used by Engel, Zhang, et al. in 1997 and gave an absolute measure of cortical responses to contrast in a single direction in color space. In these experiments the contrast was presented to the entire field (Figure 1c).
2. Upper-lower field contrast addition (Figure 1b). In the second type of experiment, we kept C1 constant over the entire array while adding and removing C2 alternately to the bottom six or top six rows of the spatial grid for periods of 24 seconds (total cycle time 48 seconds). For example, in the condition where C1 was L + M + S (luminance) contrast and C2 was L − M (red-green) contrast, the stimulus appeared as an updating achromatic checkerboard for 24 seconds and an updating checkerboard with patches that had both red/green and achromatic contrast for 24 seconds.
3. Full field contrast addition (Figure 1c). In the third type of experiment, we added C2 to the full field for 24-second periods alternating with 24 seconds of pure C1.

In a single imaging run, each 48-second cycle was repeated six times with an additional 12 seconds of discarded data at the beginning of the run to yield a total time of 5 minutes. Each condition was run at least four times in each imaging session and data from multiple runs of the same condition were averaged to improve the signal-to-noise ratio.

MRI post-processing

BOLD functional data (T2*-weighted) were collected with an in-plane resolution of 1 × 1 mm and a slice thickness of 2 mm. Anatomical in-planes (T1-weighted) were collected in the same imaging session so that the functional data could be aligned to a high-resolution (0.5 × 0.5 × 0.5 mm) structural anatomy. Functional data sets collected within a scan session were motion corrected for within- and between-scan motion. Motion was minimized across the long duration of the scanning session (8 hours) by the use of well-stabilized, anesthetized preparations.

No additional spatial or temporal filtering was applied to the fMRI time-series data beyond that imposed by the physics of the data acquisition protocol.

Dependent measures

We estimated the amplitude of the responses to different stimulus types in two ways. First, we computed the coherence between the signal in each voxel and a harmonic function at the stimulus block design frequency. This technique has been described by our group and others (e.g., Bandettini, Jesmanowicz, Wong, & Hyde, 1993; Brewer et al., 2002; Engel, Zhang, et al., 1997; Press, Brewer, Dougherty, Wade, & Wandell, 2001). Coherence is a phase-insensitive measure of signal-to-noise at the stimulus alternation frequency. The coherence level can be converted directly into a probability score under some reasonable assumptions about the spatiotemporal noise distribution (Bandettini et al., 1993).

Second, we measured the mean amplitude of the fMRI response to a single stimulus cycle. This is conceptually similar to the first statistic but yields an absolute measure of the BOLD response triggered by each stimulus type.

For both coherence and amplitude measurements, signals were projected onto a reference response phase (Boynton, Demb, Glover, & Heeger, 1999). These "phase-projected' measures are signed scalar quantities with a mean of zero. Phase-projection reduces the contribution of noise that has a random phase distribution.

Human studies

We measured fMRI data in seven human subjects. Five of these subjects also underwent retinotopic mapping experiments in separate experiments. Scanning procedures were similar to those described in Wade et al. (2002). Briefly, data were collected on a 3T GE Signa system using a posterior-head surface coil. Retinotopic mapping data were collected on all subjects prior to the onset of the study described here and visual field maps were defined using techniques described in many other publications from our laboratories (Brewer et al., 2005; Dougherty et al., 2003; Engel, Glover, & Wandell, 1997; Wade et al., 2002; Wandell, 1999). The retinotopic mapping data from all human subjects are shown in the supplementary material. Chromatic response data were measured in the regions of interest (ROIs) located within these visual field maps.

MRI parameters

fMRI data were acquired using a two-shot gradient-recalled imaging sequence incorporating an interleaved spiral K-space sampling trajectory (Noll, Cohen, Meyer, & Schneider, 1995). Volumes of 21 slices were collected, each with a field of view of 240 × 240 mm on a 128 × 128 matrix (2 × 2 mm in-plane resolution) and 3-mm slice thickness with a flip angle of 90°. The TR for each shot was 1500 msec and the effective TR for the 2-shot acquisition was 3000 msec. The near-coronal slice prescription was adjusted for each subject so that it covered the entire occipital lobe and a large part of the parietal cortex. Each experimental run consisted of 50 TRs (150 seconds) of data; data from the first 6 seconds (2 TRs) were discarded to allow the scanner to reach equilibrium.

Visual display system

Stimuli were displayed on a LCD screen within an electromagnetically shielded box placed at the foot of the scanner patient bed. Subjects viewed an image of the screen pair through binoculars that were adjusted for optimal focus and field of view at the start of every session. For all subjects, the diagonal field of view was approximately 20°. The LCD monitor was calibrated using a spectrophotometer (USB2000, OceanOptics, Dumoulin, FL). Its temporal response properties were well within the tolerances of the stimuli used in these experiments.

Stimuli

The stimuli used in the human experiments were a subset of those used in the macaque experiments. This subset corresponded to the third experiment type (full-field contrast addition) described above and illustrated in Figure 1c. The two contrast addition types used for human subjects were

1. 24% (L + M + S)-cone contrast vs. 6% (L − M)-cone + 24% (L + M + S)-cone contrast (adding chromatic contrast)
2. 6% (L − M)-cone contrast vs. 6% (L − M)-cone + 24% (L + M + S)-cone contrast (adding luminance contrast).

Stimuli were presented in a standard fMRI block design with a 50% duty cycle and a period of 24 seconds. A total of six cycles of each type of stimulus was presented in each run. In all other respects (field of view, spatial and temporal update frequency), the human stimuli were identical to those used for the macaques.

MRI post-processing

The human data, like the macaque data, were processed mainly using VISTA fMRI analysis package (http://white.stanford.edu/software). After image reconstruction and motion correction, three experiments of each contrast type were averaged to improve the signal to noise ratio in the subsequent data analysis. Phase-projected amplitudes were extracted from retinotopically defined regions of interest and these values were averaged across observers and hemispheres to compute a group mean and standard error (Figure 7).

We performed one additional analysis to investigate the hypothesis that hV4 has a color-responsive dorsal component. Visual field maps are difficult to identify in the location of this putative region and it is therefore hard to define reliable regions of interest corresponding to hV4d in different subjects (Hansen et al., 2007; Larsson & Heeger, 2006; Tootell & Hadjikhani, 2001). Moreover, chromatic responses in ventral cortex are very strong; but they are much weaker or absent in dorsal cortex. In fact, we cannot reliably identify such responses in single subject data (e.g., Figure 6). To make a best effort to identify dorsal chromatic responses, we used a surface-based averaging procedure to combine data from many subjects and search for the chromatic responses proposed to be hV4d (Hansen et al., 2007). Specifically, we generated statistical maps of phase-projected coherence generated in VISTA tools and converted them to a format that could be read by the Freesurfer analysis suite (http://surfer.nmr.mgh.harvard.edu/). We used Freesurfer routines to average data across subjects by aligning white-matter curvature maps on a spherical representation of the cortical mesh (Dale, Fischl, & Sereno, 1999; Fischl, Sereno, & Dale, 1999; Fischl, Sereno, Tootell, & Dale, 1999). Because the projected coherence is signed with zero mean, this is an effective measure for increasing the statistical power of our imaging technique. Surface-based averaging procedures respect the sulci and gyri of the cortical manifold and improve signal localization on the gray matter compared to volume-based inter-subject averaging procedures such as those requiring spatial normalization to Talairach space.

Dependent measures

The dependent measures for individual human subjects were the same as those for our macaque studies.

Results

Macaque

Retinotopic mapping

The eccentricity and polar angle maps from a single, typical monkey are shown in folded and unfolded cortex in Figures 2a and 2b. These maps are comparable to those measured by Brewer et al. (2002). We used these maps,

along with probabilistic maps of macaque visual cortex (Van Essen et al., 2001) and well-defined anatomical landmarks (for example, the lip of the operculum) to demarcate the borders of visual areas V1, V2, V3, V4, V3A, and MT. In defining retinotopic visual areas, we ensured that the polar angle and eccentricity maps were locally orthogonal as far as possible (although in some data sets, this orthogonality is sometimes distorted on a global scale; see, e.g., V4d in Figure 2).

We analyzed upper (ventral) and lower (dorsal) regions of interest within macaque V1 separately; this permits us to compare V1 responses with other quarterfield representations. The arrangement of visual areas on the posterior bank of the middle temporal gyrus is of particular interest to us. We emphasize three aspects of these maps: First, the visual field maps agree with those defined by Van Essen et al. (2001). Second, mV4 covers much of the posterior bank of the middle temporal gyrus extending from the crown of the gyrus to the base of the lunate sulcus. Third, we see hints of three separate foveal representations: One large confluence contains the foveal representations of areas V1, V2, V3, and V4 (V3/P barely extends into this confluence but we include it in these 'first tier' visual areas for convenience). In addition to this large foveal confluence, areas MT and V3A contain separate foveal representations in agreement with the literature (Fize et al., 2003).

Van Essen et al. (2001) define two small areas anterior to V4: V4ta and V4tp. We cannot distinguish separate visual areas for these regions in our data but we note that they lie on the anterior bank of the middle temporal gyrus and are likely to be encompassed by our definition of area MT. In addition, we note that an additional area: V4A defined by Zeki (1971), and likely corresponding to the region 'DLr' defined by Cusick and Kaas (1988), lies within our definition of mV4.

V1, V2, and mV4 responsivities are highest to (L − M) red-green contrast

We wanted to compare the general chromatic fMRI responses in macaque cortex with those obtained in human. To do this, we presented blocks of dynamic chromatic or achromatic contrast alternating with blocks of blank gray screen (Engel, Glover, et al., 1997; Liu & Wandell, 2005). These stimuli are likely to activate a large proportion of neurons in visual cortex. By comparing the amplitudes of responses to L − M and L + M + S chromatic contrast, we gauge the general chromatic responsivity of each visual area. We show the response time series along with a representation of the ROI locations in Figure 3.

The V1 responses to (L − M)-cone contrast are approximately double the responses to (L + M + S) contrast. Areas V2 and mV4 show a similar response profile. Areas MT and V3A show a different chromatic tuning profile, with lower (MT) or non-existent (V3A) tuning bias for chromatic stimuli.

This pattern matches measurements in human visual field maps (Engel, Glover, et al., 1997; Liu & Wandell, 2005; Wade et al., 2002). For example, several groups report that human V1 responses to L − M contrast is substantially higher than responses to L + M + S contrast (Engel, Glover, et al., 1997; Kleinschmidt, Lee, Requardt,

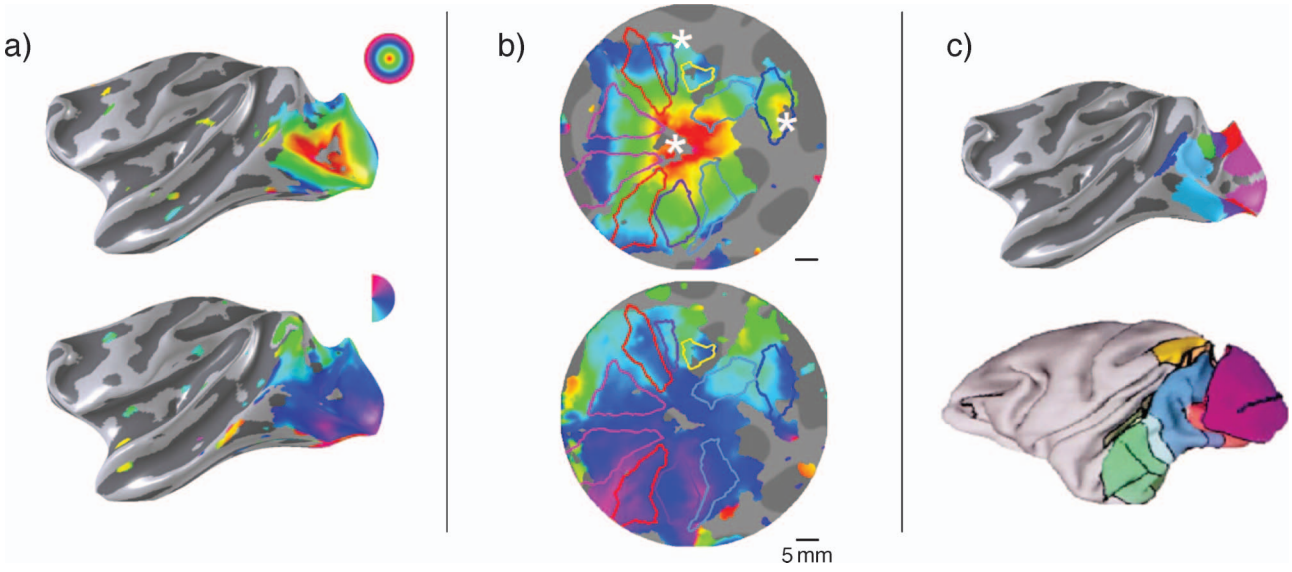

Figure 2. (a) Retinotopic mapping data on a single hemisphere (top—eccentricity map, bottom—polar angle map). (b) These data are projected onto a flattened representation of the visual cortex so that visual area can be defined. (c) The locations of these early visual areas match those in the probabilistic map from Van Essen et al. (2001). In particular, area V4 covers a large part of the posterior bank of the middle temporal gyrus and extends to the top of the gyrus. For technical reasons, visual areas are not well distinguished in the foveal confluence and so this region is undifferentiated.

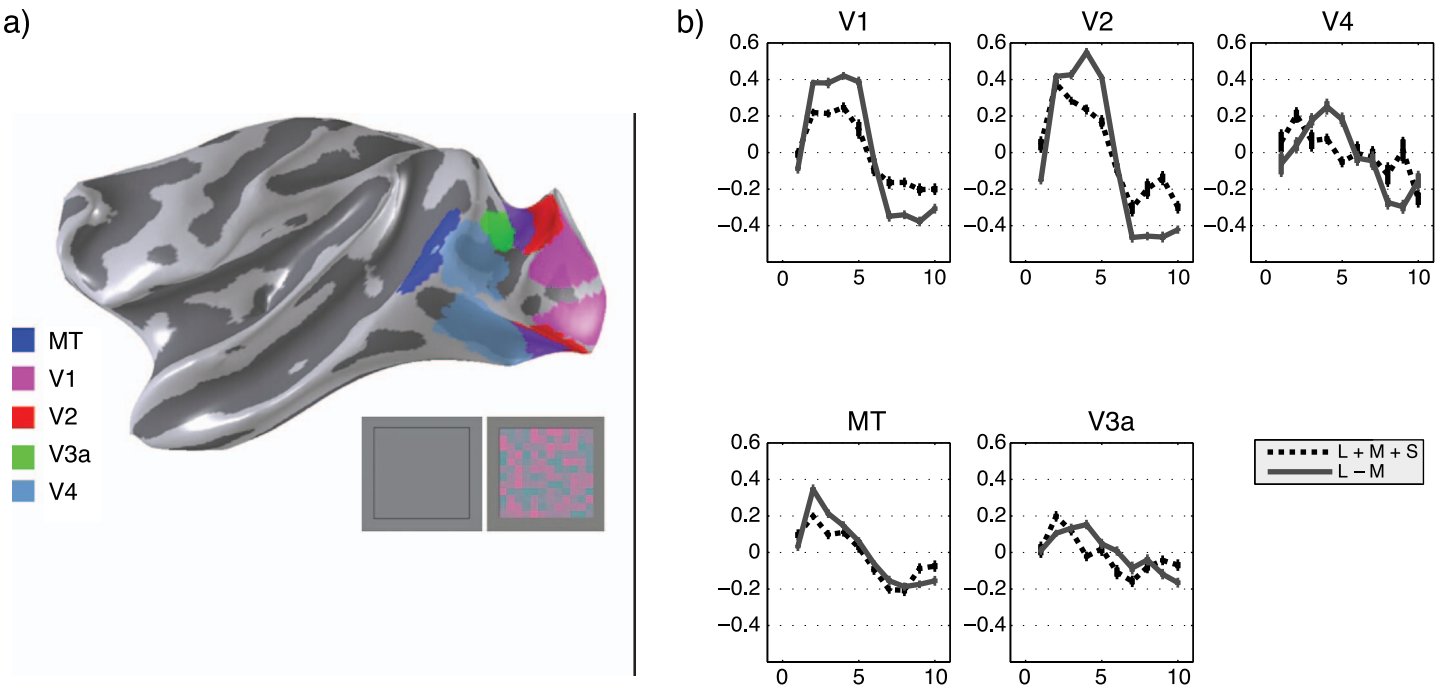

Figure 3. Average of 7 hemispheres. On/off response modulations to contrast-equated L − M and L + M + S cone stimuli in two groups of visual areas. (a) Inflated macaque cortex indication of the position of the regions of interest. (b) Mean single-cycle BOLD time series responses to the presentation of (L + M + S)-cone (dotted line) and (L − M)-cone (solid line) dynamic contrast vs. a blank mean field. The responses in V1, V2, and V4 are significantly more sensitive to L − M than L + M + S. In visual area maps V3A and MT, the responses are approximately equal.

& Frahm, 1996; Liu & Wandell, 2005). This difference to the increased sensitivity to (L − M)-cone stimuli qualitatively matches measurement in psychophysical experiments (Engel, Glover, et al., 1997; Wandell, 1995). The relative chromatic responsivity can be expressed as a ratio between the responses to (L − M)-cone and (L + M + S)-cone stimuli. For these spatiotemporal conditions, the ratios for V1 and mV4 are both just slightly less than 2:1.

We compare the responses in multiple visual areas to stimuli from two axes in cone contrast space, using the bar plots in Figure 4. Each group of bars represents data from a different visual field map. The dark gray bars are the phase-projected response amplitudes to 10% cone contrast in the (L − M)-cone direction of color space. The light gray bars are the responses to 10% 'achromatic luminance' (L + M + S)-cone contrast. Data are combined from two hemispheres of the one monkey

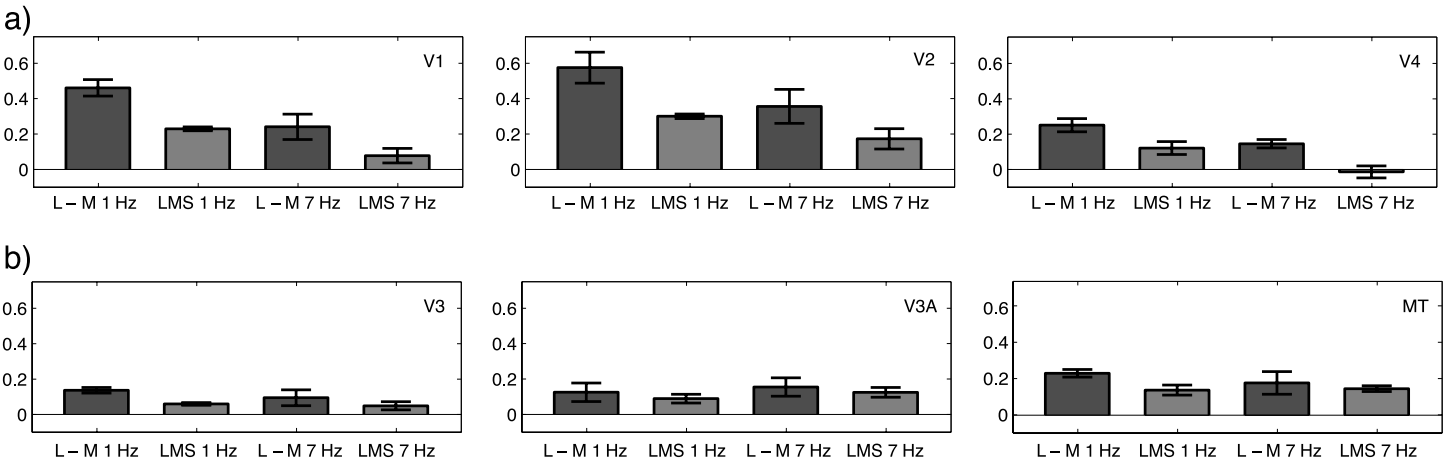

Figure 4. Comparison of BOLD response amplitude at 1 Hz and 7 Hz flicker rates. Responses to opponent (L − M)-cone and (L + M + S)-cone contrast stimuli are shown. Data are from a single monkey (averages of left and right visual areas). (a) Responses measured in areas V1, V2, and V4. (b) Responses measured in V3, V3a, and MT.

measured in different, interleaved experiments over a 12-hour period.

Extrastriate areas have different temporal-chromatic tuning

At the single-unit level, chromatic tuning measured by action potentials depends on the temporal and spatial frequencies (Solomon & Lennie, 2005; Solomon et al., 2004). This is true of the fMRI signal, as well. Figure 4 compares the (L − M) and (L + M + S) response amplitudes at 1 Hz and 7 Hz. Note that for each color, the high temporal frequency responses are generally reduced in V1, V2, and mV4 (Figure 4a). In particular, note that the mV4 response to (L + M + S) at 7 Hz is below our instrumental sensitivity. Comparing within colors, the 1-Hz and 7-Hz response amplitudes are more nearly equal in V3, V3a, and MT (Figure 4b), consistent with the temporal frequency tuning data in human ventral visual areas (Liu & Wandell, 2005).

Dorsal and ventral subregions of mV4 respond equally to color exchanges

To compare the chromatic tuning in dorsal and ventral mV4, we used a stimulus in which one dimension of dynamic cone contrast was always present (for example, (L + M + S)-cone contrast) and a second dimension (for example (L − M)-cone contrast) was turned on or off using a block design (see Figure 1b). The advantage of this experimental design is that we selectively modulate neurons tuned to the chromatic dimension of interest. Other aspects of the stimulus (including its texture and the presence or absence of an object) are constant throughout the experiment.

The time series acquired from eight small regions of interest located at five degrees eccentricity in four visual areas of a single cortex are compared in Figure 5. In this experiment, opponent color (L − M)-cone contrast was added alternately to the lower, then the upper visual field. The time series in Figure 5b show a single cycle of data for each area. The time series combine the data from left and right hemispheres; they are also averaged across

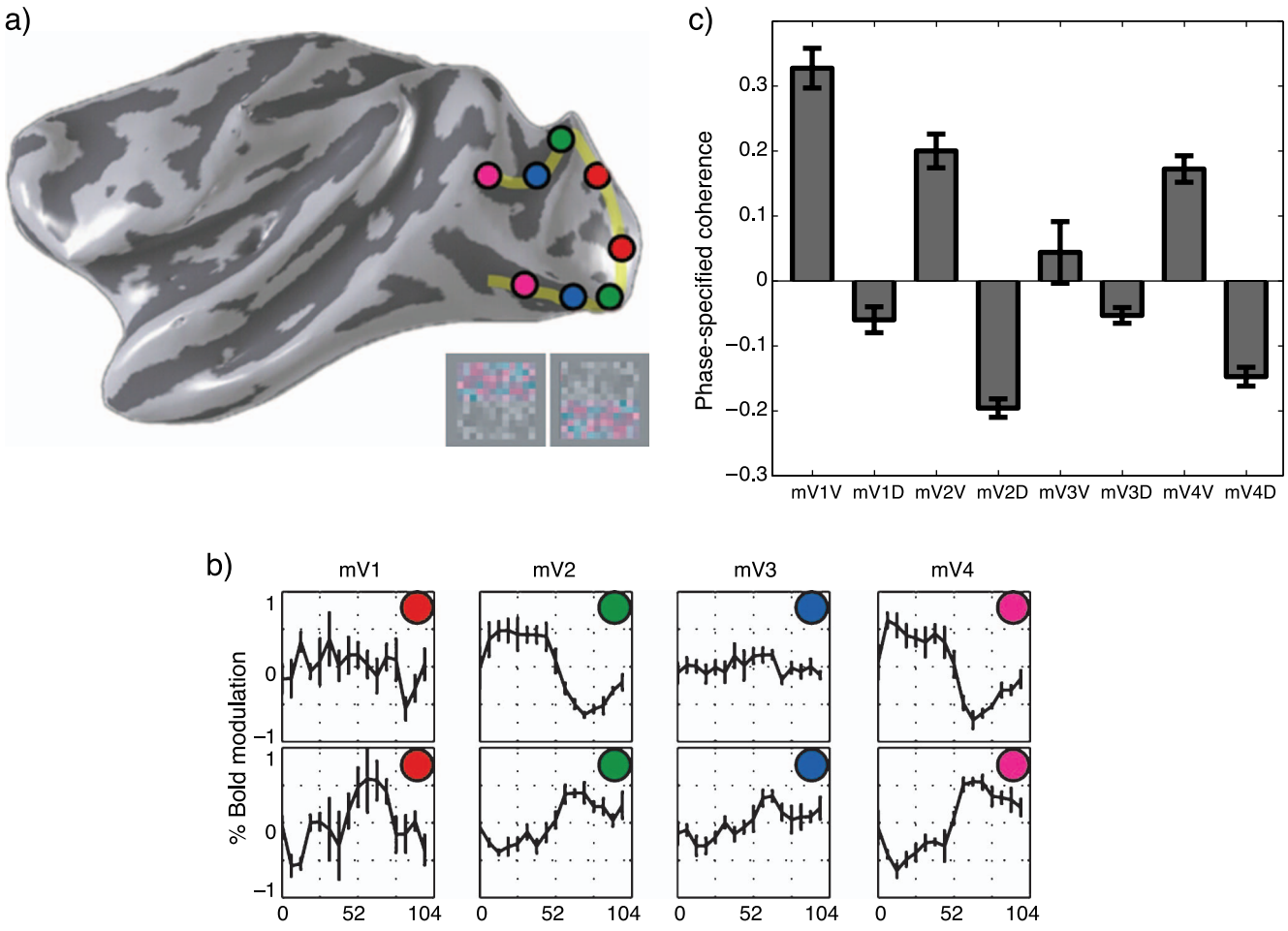

Figure 5. Comparison of upper and lower visual field modulations averaged across 5 macaque hemispheres. (a) Rendered view of macaque cortex showing locations of circular ROIs defined at 5 degrees eccentricity. (b) Mean time BOLD time series of responses in the dorsal and ventral parts of areas V1, V2, V3, and V4. Note the similarity both in amplitude and shape of the responses in V4d and V4v. (c) Bar plot of phase-specified coherence in each ROI. Negative values indicate responses to contrast additions in the lower visual field.

stimulus cycles. In this animal, we found the largest responses to chromatic contrast in areas V2 and V4. Dorsal areas (mV2d, mV4d) show responses in the first half of the stimulus cycle, consistent with receptive fields covering the lower visual field. Ventral areas (mV4v, mV2v) respond maximally in the second half of the stimulus cycle when the chromatic contrast was present in the upper visual field. On average we see a similar pattern of results across all the monkeys we scanned. In two out of three animals, we found significant activation in area V1 as well as in the extrastriate areas. The presence of significant noise in V1d in one monkey reduced the apparent similarity between the dorsal and ventral responses in this area but the functional unity of primary visual cortex is well established.

In most regions responding strongly to the addition of color contrast, the dorsal and ventral subdivisions respond equally. By this measure, dorsal macaque V4 and ventral macaque V4 could be part of the same functional area, in contrast to recent reports (Fize et al., 2003). These results support the hypothesis that electrophysiological measurements from mV4d would be similar to those obtained from mV4v (Zeki, 1983).

Human

In humans, color exchanges primarily activate V1 and ventral areas

A variety of experiments have shown that extrastriate human color responses are largely confined to the ventral surface (Bartels & Zeki, 2000; Hadjikhani et al., 1998; Wade et al., 2002; Zeki et al., 1991). However, in macaque, robust chromatic responses can be measured in dorsal mV4 (Figure 5).

We wondered whether the particular stimuli used in our experiments generate spatial responses similar to those reported by other groups (for example, a strong bias for isoluminant (L − M)-cone contrast in primary visual cortex). In addition, if we measure significant chromatic responses in a ventral hV4 region, we would expect to measure a similar chromatic response in a putative dorsal counterpart. Finding such an 'island' of chromatic responsivity on the dorsolateral surface near area V3d would support the 'vestigial hV4d' hypothesis of Hansen et al. (2007).

To address these questions, we carried out full-field versions of the chromatic color exchange experiment to identify cortical regions that responded preferentially to the addition of 1 Hz, 6% (L − M)-cone contrast in the presence of a constant 24% contrast luminance modulation (see Figure 1c). Figure 6a shows a typical result from these experiments: There are strong responses to chromatic contrast on the ventral surface within and anterior to area hV4; there are also weaker but significant responses in V1 and V2. The responses within hV4 are mainly

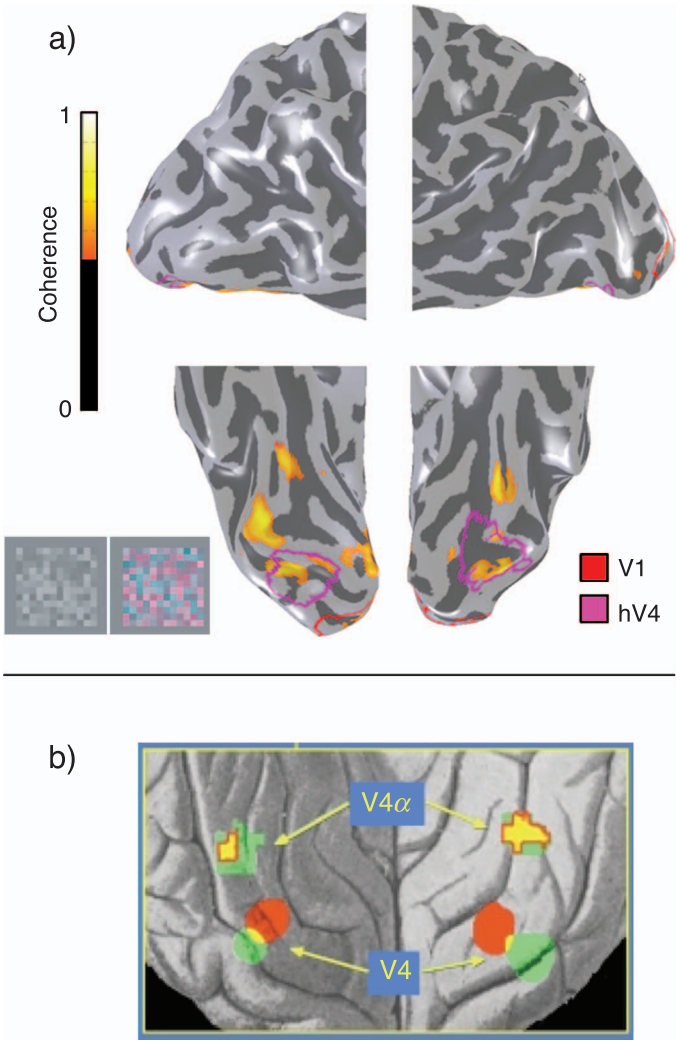

Figure 6. Human data. (a) Typical response to the addition of 6% RMS (L − M)-cone contrast to a 24% RMS (L + M + S)-cone contrast grating in a single subject. (b) Figure 1 from Zeki and Bartels (1999) showing group average response to chromatic vs. achromatic Mondrian stimulus.

located in the relatively peripheral portion of the map. This is expected because the patch sizes are rather large, thereby biasing the response to neurons that prefer low spatial frequency. It is instructive to note the similarity of this figure (as well as Figure 7) to that measured by Zeki and Bartels in 1999 reproduced here in Figure 6b. Our hV4 area is essentially identical to their 'V4' and the more anterior activation in our data corresponds to their 'V4α.'

In single-subject analyses, we could find no significant responses to the color exchange on the lateral or dorsal surfaces. These experiments confirm the oft-repeated observation that the most powerful extrastriate fMRI responses to low spatiotemporal frequency chromatic contrast are located in ventral human visual areas.

In Figure 7 we show the results of a more powerful group analysis. Figure 7a shows the results of a surface-based average of 7 observers (Fischl, Sereno, Tootell,

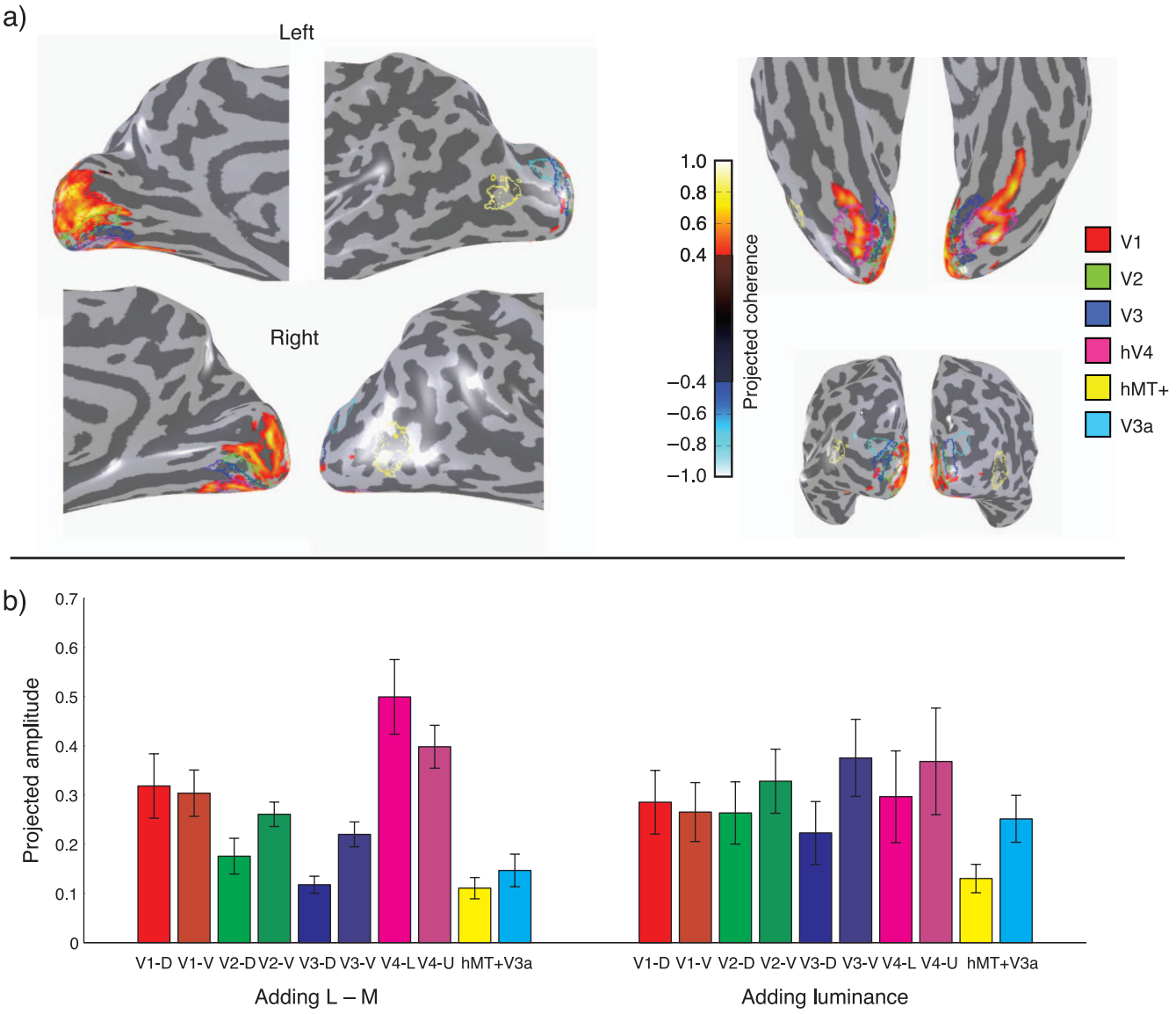

Figure 7. Human data. (a) Surface-averaged projected coherence maps from 7 subjects showing mean response to chromatic contrast addition. Responses are primarily in striate cortex and on the ventral surface anterior to V3V. (b) ROI analysis of chromatic and achromatic contrast addition experiments in five subjects. Left panel shows mean projected amplitudes of responses to 6% chromatic contrast addition. Right panel shows responses to 24% achromatic contrast condition. Both the upper and lower visual fields of area hV4 respond more strongly than V1 to the addition of chromatic contrast. In comparison, hV4 is no more sensitive to luminance contrast than other retinotopic, extrastriate visual areas.

et al., 1999). Projected coherence maps from the same chromatic contrast addition experiments as those used to generate Figure 6 were averaged across seven subjects. The resulting mean projected coherence maps are shown on a reference brain with retinotopic regions of interest V1, V2, V3, V3a, hV4, and hMT+ overlaid. Despite the relatively low coherence threshold (equivalent to a probability value of 0.001), responses are still largely confined to primary visual cortex and ventral areas. Figure 7b shows an ROI-based analysis of the same data set (left panel) as well as a similar data set in which pure luminance contrast (24%) was added to a constant level of chromatic contrast (right panel).

Although they are measured in different species, in different scanners and under very different attentional states, it is interesting to compare chromatic responses in human and macaque visual areas. Firstly, in both species, the amplitudes of responses to chromatic contrast in areas hV4d and hV4v are higher than the neighboring area V3. This contributes to the appearance of hV4 as an 'island' of activation on the ventral surface of human visual cortex and separates V4 from V2 in macaques. Secondly, in both species, V1 exhibits a robust response to the addition of chromatic contrast. In macaques, it is the area with the strongest response. In humans it has the second highest amplitude after hV4. Thirdly, in macaques, area V2

responds more strongly to chromatic contrast than area V4. In humans, hV4 shows the strongest response of all the retinotopic visual areas measured. V2 in macaque is known to contain stripes sensitive to both chromatic and achromatic contrast (Xiao, Wang, & Felleman, 2003), and we hypothesize that this difference may be due to the relatively low spatial resolution of our human data which necessarily blurs together responses in these two subdomains. Finally, the responses to luminance contrast addition are very similar across visual areas and hV4 shows no particular preference for this stimulus compared to its neighbors.

The single most striking observation is that in both macaque and humans, both visual fields of hV4 respond strongly to chromatic contrast and have similar response amplitudes. This suggests that in both species, these two visual fields form a single, functionally unified visual area. In humans this visual area is confined to the ventral surface while in macaque is split evenly between the dorsal and ventral surfaces.

Does human V4 extend onto the lateral surface?

Hansen and Gallant proposed that human V4 is largely but not entirely confined to the ventral surface. Specifically, they suggest that a thin strip of visual cortex adjacent to V3d contains a representation of the lower visual field that should be paired with a near-hemifield representation in hV4 on the ventral surface.

If this hypothesis is correct, we expect to measure a small but significant response to chromatic contrast addition in this location since we have already shown that the ventral hV4 responds strongly to this stimulus. In fact, the surface-based average shown in Figure 7a and in more detail in Figure 8 shows some hints of response in this location (circled) but these activations are barely above threshold. The fact that they do achieve statistical significance and appear bilaterally in the approximate location of the region proposed by Hansen and Gallant is intriguing but we do not believe that there is sufficient evidence to support conclusively the 'vestigial V4d' hypothesis at this point.

Discussion

These experiments advance our understanding of the relationship between human and macaque cortical color representations in four ways. First, macaque color tuning in primary visual cortex is qualitatively similar to that measured in human. In area V1, the sensitivity to 1 Hz (L − M)-cone contrast is between two and four times the sensitivity to (L + M + S)-cone contrast.

Second, as in humans (Liu & Wandell, 2005) the chromatic responses in macaque depend critically on the temporal frequency of the stimulus. Area mV4 responds preferentially to low temporal frequency signals, and it has very little responsivity at 7 Hz. These responses are consistent with human color perception.

Third, macaque responses to the color exchange stimulus are located on both the dorsal and ventral components of mV4, and the chromatic responses in the dorsal and ventral portions of mV4 are similar. Hence, for these stimuli and at this level of spatial resolution, dorsal and ventral mV4 appear to be part of a single, functionally homogeneous visual hemifield representation. It is possible, of course, that one might find differences in the dorsal

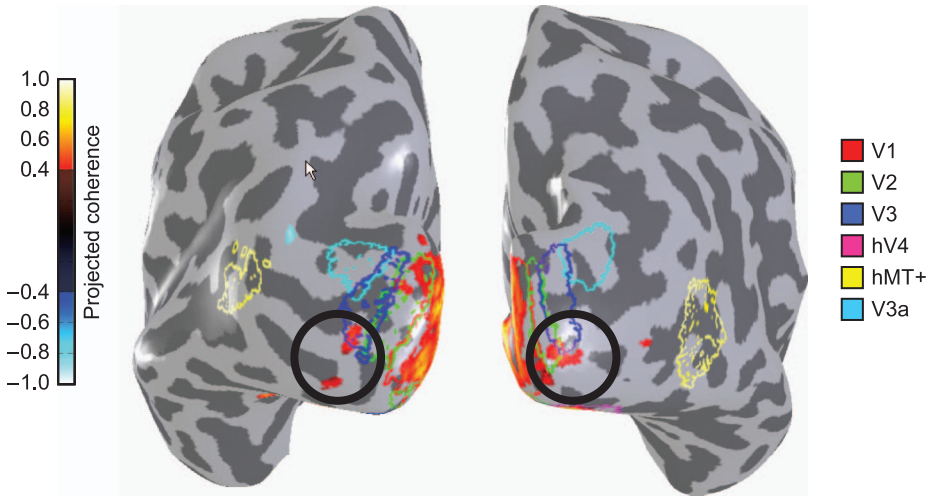

Figure 8. Detail from Figure 7a showing posterior visual cortex. Bilateral regions with weak super-threshold responses to chromatic contrast are circled. These regions are in locations that make them candidates for the human V4d homologue proposed by Hansen and Gallant.

and ventral circuitry at some higher resolution. But we add that the coarse functional measurements described here are consistent with recent single-unit recordings showing that there is similar color selectivity in ventral mV4 (Kusunoki, Moutoussis, & Zeki, 2006). Further, perfect correspondence between dorsal and ventral responses is probably too demanding a requirement. There are many differences of physiological responses within maps that do not rise to the level of requiring a subdivision; one of many well-known examples is the differences in receptive field size when comparing fovea to periphery (Van Essen, Newsome, & Maunsell, 1984). The responsivity to color exchanges provides no compelling evidence that the dorsal and ventral portions of mV4 differ. The measurement technique has adequate sensitivity to identify certain differences, such as the very different sensitivity in the neighboring map, V3. The color-exchange measurements here support the proposition that these two portions of mV4 share common neural circuitry that is responsive to color (Zeki, 2003).

Fourth, unlike macaque, extrastriate human responses to the color exchange stimuli are largely confined to the ventral surface of the occipital lobe. These responses fall within hV4 as well as anterior regions on the ventral surface.

Quarterfield and hemifield achromatopsia and white matter

If we accept that hV4 represents nearly an entire hemifield, we are left with a puzzle. The literature includes several convincing cases of a sharp quarterfield achromatopsia (Kölmel, 1988; Merigan, Freeman, & Meyers, 1997) as well as cases of a hemifield achromatopsia. In their review paper, Bouvier and Engel (2006) explain quarterfield achromatopsias by supposing that human ventral surface contains a quarterfield and hemifield map. The puzzle stems from the fact that recent neuroimaging data show that the hV4 map represents significantly more than a quarterfield—either an entire hemifield representation or close to it (Brewer et al., 2005; Hansen et al., 2007; Merabet et al., 2007; Wandell et al., 2007). The data further show that hV4 responds relatively strongly to chromatic contrast. If this strong activation indicates a functional dependency, we would expect damage to hV4 to generate achromatopsia but only very rarely would this achromatopsia be confined to a cleanly delineated quarterfield.

One way to reconcile these findings is to consider the physical paths taken by the neurons that connect hV4 to earlier retinotopic areas. The axons carrying information about the upper and lower visual field come from widely separated locations. The upper-field signals originate in V1v/V2v and V3v, adjacent to hV4. The lower-field signals originate in V1d/V2d and V3d, several centimeters away from hV4. A stroke that damages the ventral axons, sparing the dorsal V1/V2/V3 axons, deprives hV4 of its upper visual field representation. Such damage could result in a sharp quarterfield achromatopsia. This hypothesis allows the ventral gray matter map to represent significantly more than a quarterfield; it explains the sharp quarterfield loss by attributing the damage to the distinct white matter inputs. In the future, this hypothesis could be tested by identifying and tracing the different fiber pathways projecting to the ventral hemifield maps.

Responses outside mV4 and hV4

While we did not measure reliable color-exchange responses anterior to mV4 in macaques, the absence of such signals is almost surely a limitation of our methods: we measured a restricted field of view using relatively small surface coils and the animals were anesthetized. fMRI in the awake animal shows robust activation at foci slightly anterior to mV4 in response to chromatic gratings (Conway, Moeller, & Tsao, 2007). Activation in these regions in response to chromatic stimuli has also been measured using 2-deoxyglucose uptake (Tootell, Nelissen, Vanduffel, & Orban, 2004). Such activation is expected because earlier single-unit experiments also report a high density of color-selective neurons in these ventral anterior regions (Zeki, 1973). In his original work, Zeki proposed that these anterior regions are part of a ‘color complex.’ The naming conventions for this region are not uniform across laboratories and it contains locations referred to as V4A, PIT, DLr, and posterior TEO by different investigators (Distler, Boussaoud, Desimone, & Ungerleider, 1993; Felleman, Xiao, & McClendon, 1997; Stepniewska & Kaas, 1996; Zeki, 1996).

The activations in Conway et al. (2007) also show that V1 is more responsive to zero luminance-contrast red-blue gratings than to luminance-contrast gratings. Also in agreement with our measurements, in awake macaque monkey they find that the only significant responses in dorsal cortex are in mV4d or right on the border of mV4d (see Figure 2 of Conway et al., 2007).

The perceptual significance of these responses remains an open question. As many researchers have pointed out, lesions of mV4 do not eliminate the animal’s ability to make certain fundamental color judgments (Heywood et al., 1992; Walsh et al., 1993; Walsh, Kulikowski, et al., 1992). Certain color discrimination capabilities also remain in cases of human cerebral achromatopsia (Heywood, Cowey, & Newcombe, 1991; Kennard et al., 1995; Mollon et al., 1980). While some color discrimination capabilities are preserved in spite of these lesions, it appears that color perception in general, and color constancy in particular is disturbed (Kennard et al., 1995; Walsh et al., 1993). Lesion studies therefore support the idea that many computations fundamental to color vision occur prior to V4 in the processing hierarchy.

Color responsive cortex

At the spatial resolution of fMRI, there is a fundamental asymmetry between color and luminance selective regions: most of visual cortex responds to achromatic luminance contrast but there are cortical regions that are not highly responsive to the other two color dimensions. At the higher resolution of single-units, it may be possible to identify additional clusters of luminance and chrominance selective cortex (Conway et al., 2007).

Very few regions appear to be entirely *unresponsive* to color. Even area MT; part of the archetypal, luminance-driven, dorsal pathway, contains many cells that are driven by zero luminance (L − M)-cone contrast and even some driven by pure S-cone contrast (Barberini, Cohen, Wandell, & Newsome, 2005; Liu & Wandell, 2005; Seidemann, Poirson, Wandell, & Newsome, 1999). No complete visual field map has been found that responds **only** to zero luminance color contrast.

The origins of this observation may lie in the chromatic tuning properties of V1 neurons. Careful measurements of the chromatic tuning of V1 neurons in recent years have demonstrated that only a minority (roughly 10%) of neurons in this area respond exclusively to chromatic contrast. These purely color-selective neurons tend to be spatially low-pass and have weak orientation tuning. Interestingly, their chromatic tuning properties are relatively invariant with respect to stimulus contrast and size (Solomon & Lennie, 2005; Solomon et al., 2004).

The preponderance of neurons in primary visual cortex respond to pure isoluminant stimuli, and roughly half are sensitive enough to both luminance and isoluminant stimuli that they are classified either as 'color-luminance' cells or as luminance-preferring cells with some cone opponency (Conway, 2001; Johnson et al., 2001, 2004). Unlike the neurons that respond exclusively to chromatic contrast, the chromatic tuning of these mixed neurons depends both upon the contrast and size of the stimulus (Solomon & Lennie, 2005; Solomon et al., 2004).

The different types of neurons may contribute to different functional aspects of color vision. It is possible, for example, that identifying an object's color may depend on signals from color-selective neurons while detecting and analyzing chromatically defined forms and textures necessarily depends more on orientation-tuned cells which have weaker and slightly less stable color tuning (Gegenfurtner, 2001). The reports of achromatopsic subjects with ventral visual cortex lesions surface seem to suggest that their deficits lie more in the first type of color processing than the second—in other words, their conscious perception of chromatic identity is disrupted but they often have little difficulty in detecting and discriminating visual features defined solely by isoluminant color boundaries. In fact, one study reports that an achromatopsic patient who failed to detect figures in Ishihara plates presented at short range could complete the task when the same plates were presented at a distance, presumably because the former task required a higher-level assignment of chromatic identity across visual distances greater than that spanned by a single V1 receptive field while the latter task required only the detection of local chromatic borders (Mollon et al., 1980). This observation also serves as a reminder that our perception of a stimulus' color is fundamentally dependent upon its spatiotemporal frequency as well as its cone contrast ratio.

The stimuli used in our experiments contained many chromatic boundaries. If we accept the extensive evidence that mV4 has a significant role in form processing (Desimone, Schein, Moran, & Ungerleider, 1985; Gallant, Connor, Rakshit, Lewis, & Van Essen, 1996; Hegdé & Van Essen, 2007; Merigan, 1996; Pasupathy & Connor, 2002; Walsh, Butler, Carden, & Kulikowski, 1992), it is possible that much of the apparent V4 chromatic sensitivity in both macaques and humans is driven by pathways originating with the color-luminance cells in V1 that are sensitive to spatial patterns. In addition, it may be that that V4 integrates information about form and chromatic identity, combining signals from both color-luminance and color-selective pathways. It would follow that V4 lesions in both humans and macaques should result in joint chromatic and form-processing deficits. In line with this hypothesis, we note that upon careful testing, almost all human achromatopes show some deficits in form processing (Bouvier & Engel, 2006; Gallant, Shoup, & Mazer, 2000) and there is evidence that lesions to areas including V4 in macaques generate significant deficits in both form and color processing (Walsh, Butler, et al., 1992). Therefore, one explanation for the strong response of V4 to chromatic stimuli may be that it is one of the first areas to inherit and process information from both populations of chromatically sensitive cells in V1. This apparent sensitivity may be enhanced by the general trend towards contrast invariance in higher-order visual areas (Avidan et al., 2002; Tjan, Lestou, & Kourtzi, 2006).

Summary

The fMRI responses in human and macaque V4 to Mondrian color addition are qualitatively similar. The responses are consistent with the hypothesis that at least some of the signals in these maps are used to estimate and represent color appearance or identify chromatically defined features, although the apparent chromatic sensitivity of mV4 may be partially a function of the low temporal frequency of our stimuli as well as those used by others in the field (Hadjikhani et al., 1998). In macaque, the dorsal and ventral responses in V4 are significant and similar, suggesting that the two parts of mV4 form a single functional unit. In humans, there may be a small dorsal response to these stimuli, but the ventral component of the signal is far larger in amplitude and spatial extent and extends into both lower and upper visual field representations of a hemifield adjacent to ventral V3. This

hemifield, which we termed hV4 in previous studies, is located predominantly on the ventral surface. Functionally, it appears to be a good match to mV4, which has significant dorsal and ventral components. A predominantly ventral hV4 hemifield needs to be reconciled with the case reports of a sharp quarterfield achromatopsia; we suggest that white matter pathways deliver distinct quadrant visual field information to the ventral field maps. Damage from stroke may eliminate one of the input bundles but spare the other, thereby generating a clean quarterfield achromatopsia despite the fact that hV4 appears to represent a large proportion, if not all, of a visual hemifield.

Acknowledgments

Supported by NIH/NEI grants: EY03164, EY015790, the Max-Planck Institute, and the Smith-Kettlewell Eye Research Institute. We thank William Newsome for discussions leading to these experiments and Semir Zeki for his comments on an earlier version of this manuscript.

Figure 6b is reproduced from Zeki and Bartels (1999) with the kind permission of the authors and the publisher.

Commercial relationships: none.
Corresponding author: Alex R. Wade.
Email: wade@wadelab.net.
Address: 2318 Fillmore St., San Francisco, CA 94115, USA.

References

Avidan, G., Harel, M., Hendler, T., Ben-Bashat, D., Zohary, E., & Malach, R. (2002). Contrast sensitivity in human visual areas and its relationship to object recognition. *Journal of Neurophysiology, 87,* 3102–3116. [PubMed] [Article]

Bandettini, P. A., Jesmanowicz, A., Wong, E. C., & Hyde, J. S. (1993). Processing strategies for time-course data sets in functional MRI of the human brain. *Magnetic Resonance in Medicine, 30,* 161–173. [PubMed]

Barberini, C. L., Cohen, M. R., Wandell, B. A., & Newsome, W. T. (2005). Cone signal interactions in direction-selective neurons in the middle temporal visual area (MT). *Journal of Vision, 5*(7):1, 603–621, http://journalofvision.org/5/7/1/, doi:10.1167/5.7.1. [PubMed] [Article]

Barbur, J. L., Harlow, A. J., & Plant, G. T. (1994). Insights into the different exploits of colour in the visual cortex. *Proceedings of the Royal Society B: Biological Sciences, 258,* 327–334. [PubMed]

Bartels, A., & Zeki, S. (2000). The architecture of the colour centre in the human visual brain: New results and a review. *European Journal of Neuroscience, 12,* 172–193. [PubMed]

Baylor, D. A. (1987). Photoreceptor signals and vision. Proctor lecture. *Investigative Ophthalmology & Visual Science, 28,* 34–49. [PubMed] [Article]

Baylor, D. A., Nunn, B. J., & Schnapf, J. L. (1987). Spectral sensitivity of cones of the monkey Macaca fascicularis. *The Journal of Physiology, 390,* 145–160. [PubMed] [Article]

Bouvier, S. E., & Engel, S. A. (2006). Behavioral deficits and cortical damage loci in cerebral achromatopsia. *Cerebral Cortex, 16,* 183–191. [PubMed] [Article]

Boynton, G. M., Demb, J. B., Glover, G. H., & Heeger, D. J. (1999). Neuronal basis of contrast discrimination. *Vision Research, 39,* 257–269. [PubMed]

Brainard, D. H. (1989). Calibration of a computer controlled color monitor. *Color Research and Application, 14,* 23–34.

Brainard, D. H. (1997). The Psychophysics Toolbox. *Spatial Vision, 10,* 433–436. [PubMed]

Brewer, A. A., Liu, J., Wade, A. R., & Wandell, B. A. (2005). Visual field maps and stimulus selectivity in human ventral occipital cortex. *Nature Neuroscience, 8,* 1102–1109. [PubMed]

Brewer, A. A., Press, W. A., Logothetis, N. K., & Wandell, B. A. (2002). Visual areas in macaque cortex measured using functional magnetic resonance imaging. *Journal of Neuroscience, 22,* 10416–10426. [PubMed] [Article]

Chatterjee, S., & Callaway, E. M. (2003). Parallel colour-opponent pathways to primary visual cortex. *Nature, 426,* 668–671. [PubMed]

Conway, B. R. (2001). Spatial structure of cone inputs to color cells in alert macaque primary visual cortex (V-1). *Journal of Neuroscience, 21,* 2768–2783. [PubMed] [Article]

Conway, B. R., Moeller, S., & Tsao, D. Y. (2007). Specialized color modules in macaque extrastriate cortex. *Neuron, 56,* 560–573. [PubMed]

Cowey, A., Heywood, C. A., & Irving-Bell, L. (2001). The regional cortical basis of achromatopsia: A study on macaque monkeys and an achromatopsic patient. *European Journal of Neuroscience, 14,* 1555–1566. [PubMed]

Cusick, C. G., & Kaas, J. H. (1988). Cortical connections of area 18 and dorsolateral visual cortex in squirrel monkeys. *Visual Neuroscience, 1,* 211–237. [PubMed]

Dale, A. M., Fischl, B., & Sereno, M. I. (1999). Cortical surface-based analysis. I. Segmentation and surface reconstruction. *Neuroimage, 9,* 179–194. [PubMed]

Derrington, A. M., Krauskopf, J., & Lennie, P. (1984). Chromatic mechanisms in lateral geniculate nucleus

of macaque. *The Journal of Physiology, 357,* 241–265. [PubMed] [Article]

Desimone, R., Schein, S. J., Moran, J., & Ungerleider, L. G. (1985). Contour, color and shape analysis beyond the striate cortex. *Vision Research, 25,* 441–452. [PubMed]

De Valois, R. L., & Jacobs, G. H. (1968). Primate color vision. *Science, 162,* 533–540. [PubMed]

De Valois, R. L., Jacobs, G. H., & Abramov, I. (1964). Responses of single cells in visual system to shifts in the wavelength of light. *Science, 146,* 1184–1186. [PubMed]

DeYoe, E. A., Carman, G. J., Bandettini, P., Glickman, S., Wieser, J., Cox, R., et al. (1996). Mapping striate and extrastriate visual areas in human cerebral cortex. *Proceedings of the National Academy of Sciences of the United States of America, 93,* 2382–2386. [PubMed] [Article]

Distler, C., Boussaoud, D., Desimone, R., & Ungerleider, L. G. (1993). Cortical connections of inferior temporal area TEO in macaque monkeys. *Journal of Comparative Neurology, 334,* 125–150. [PubMed]

Dougherty, R. F., Koch, V. M., Brewer, A. A., Fischer, B., Modersitzki, J., & Wandell, B. A. (2003). Visual field representations and locations of visual areas V1/2/3 in human visual cortex. *Journal of Vision, 3*(10):1, 586–598, http://journalofvision.org/3/10/1/, doi:10.1167/3.10.1. [PubMed] [Article]

Engel, S. A., Glover, G. H., & Wandell, B. A. (1997). Retinotopic organization in human visual cortex and the spatial precision of functional MRI. *Cerebral Cortex, 7,* 181–192. [PubMed] [Article]

Engel, S. A., Rumelhart, D. E., Wandell, B. A., Lee, A. T., Glover, G. H., Chichilnisky, E. J., et al. (1994). fMRI of human visual cortex. *Nature, 369,* 525. [PubMed]

Engel, S. A., Zhang, X., & Wandell, B. (1997). Colour tuning in human visual cortex measured with functional magnetic resonance imaging. *Nature, 388,* 68–71. [PubMed]

Essen, D. C., & Zeki, S. M. (1978). The topographic organization of rhesus monkey prestriate cortex. *The Journal of Physiology, 277,* 193–226. [PubMed] [Article]

Felleman, D. J., Xiao, Y., & McClendon, E. (1997). Modular organization of occipito-temporal pathways: Cortical connections between visual area 4 and visual area 2 and posterior inferotemporal ventral area in macaque monkeys. *Journal of Neuroscience, 17,* 3185–3200. [PubMed] [Article]

Field, G. D., & Chichilnisky, E. J. (2007). Information processing in the primate retina: Circuitry and coding. *Annual Review of Neuroscience, 30,* 1–30. [PubMed]

Fischl, B., Sereno, M. I., & Dale, A. M. (1999). Cortical surface-based analysis. II: Inflation, flattening, and a surface-based coordinate system. *Neuroimage, 9,* 195–207. [PubMed]

Fischl, B., Sereno, M. I., Tootell, R. B., & Dale, A. M. (1999). High-resolution intersubject averaging and a coordinate system for the cortical surface. *Human Brain Mapping, 8,* 272–284. [PubMed]

Fize, D., Vanduffel, W., Nelissen, K., Denys, K., Chef d'Hotel, C., Faugeras, O., et al. (2003). The retinotopic organization of primate dorsal V4 and surrounding areas: A functional magnetic resonance imaging study in awake monkeys. *Journal of Neuroscience, 23,* 7395–7406. [PubMed] [Article]

Gallant, J. L., Connor, C. E., Rakshit, S., Lewis, J. W., & Van Essen, D. C. (1996). Neural responses to polar, hyperbolic, and Cartesian gratings in area V4 of the macaque monkey. *Journal of Neurophysiology, 76,* 2718–2739. [PubMed]

Gallant, J. L., Shoup, R. E., & Mazer, J. A. (2000). A human extrastriate area functionally homologous to macaque V4. *Neuron, 27,* 227–235. [PubMed] [Article]

Gattass, R., Sousa, A. P., & Gross, C. G. (1988). Visuotopic organization and extent of V3 and V4 of the macaque. *Journal of Neuroscience, 8,* 1831–1845. [PubMed] [Article]

Gegenfurtner, K. (2001). Color in the cortex revisited. *Nature Neuroscience, 4,* 339–340. [PubMed]

Hadjikhani, N., Liu, A. K., Dale, A. M., Cavanagh, P., & Tootell, R. B. (1998). Retinotopy and color sensitivity in human visual cortical area V8. *Nature Neuroscience, 1,* 235–241. [PubMed]

Hansen, K. A., Kay, K. N., & Gallant, J. L. (2007). Topographic organization in and near human visual area V4. *Journal of Neuroscience, 27,* 11896–11911. [PubMed] [Article]

Hegdé, J., & Van Essen, D. C. (2007). A comparative study of shape representation in macaque visual areas v2 and v4. *Cerebral Cortex, 17,* 1100–1116. [PubMed] [Article]

Heywood, C. A., & Cowey, A. (1987). On the role of cortical area V4 in the discrimination of hue and pattern in macaque monkeys. *Journal of Neuroscience, 7,* 2601–2617. [PubMed] [Article]

Heywood, C. A., Cowey, A., & Newcombe, F. (1991). Chromatic discrimination in a cortically colour blind observer. *European Journal of Neuroscience, 3,* 802–812. [PubMed]

Heywood, C. A., Gadotti, A., & Cowey, A. (1992). Cortical area V4 and its role in the perception of color. *Journal of Neuroscience, 12,* 4056–4065. [PubMed] [Article]

Heywood, C. A., Wilson, B., & Cowey, A. (1987). A case study of cortical colour "blindness" with relatively intact achromatic discrimination. *Journal of Neurology, Neurosurgery and Psychiatry, 50,* 22–29. [PubMed] [Article]

Howard, R. J., ffytche, D. H., Barnes, J., McKeefry, D., Ha, Y., Woodruff, P. W., et al. (1998). The functional anatomy of imagining and perceiving colour. *Neuroreport, 9,* 1019–1023. [PubMed]

Hurvich, L. M., & Jameson, D. (1957). An opponent-process theory of color vision. *Psychological Review, 64,* 384–404. [PubMed]

Johnson, E. N., Hawken, M. J., & Shapley, R. (2001). The spatial transformation of color in the primary visual cortex of the macaque monkey. *Nature Neuroscience, 4,* 409–416. [PubMed]

Johnson, E. N., Hawken, M. J., & Shapley, R. (2004). Cone inputs in macaque primary visual cortex. *Journal of Neurophysiology, 91,* 2501–2514. [PubMed] [Article]

Kennard, C., Lawden, M., Morland, A. B., & Ruddock, K. H. (1995). Colour identification and colour constancy are impaired in a patient with incomplete achromatopsia associated with prestriate cortical lesions. *Proceedings of the Royal Society B: Biological Sciences, 260,* 169–175. [PubMed]

Kleinschmidt, A., Lee, B. B., Requardt, M., & Frahm, J. (1996). Functional mapping of color processing by magnetic resonance imaging of responses to selective P- and M-pathway stimulation. *Experimental Brain Research, 110,* 279–288. [PubMed]

Kölmel, H. W. (1988). Pure homonymous hemiachromatopsia. Findings with neuro-ophthalmologic examination and imaging procedures. *European Archives of Psychiatry and Neurological Sciences, 237,* 237–243. [PubMed]

Kusunoki, M., Moutoussis, K., & Zeki, S. (2006). Effect of background colors on the tuning of color-selective cells in monkey area V4. *Journal of Neurophysiology, 95,* 3047–3059. [PubMed] [Article]

Larsson, J., & Heeger, D. J. (2006). Two retinotopic visual areas in human lateral occipital cortex. *Journal of Neuroscience, 26,* 13128–13142. [PubMed] [Article]

Liu, J., & Wandell, B. A. (2005). Specializations for chromatic and temporal signals in human visual cortex. *Journal of Neuroscience, 25,* 3459–3468. [PubMed] [Article]

Logothetis, N. K., Guggenberger, H., Peled, S., & Pauls, J. (1999). Functional imaging of the monkey brain. *Nature Neuroscience, 2,* 555–562. [PubMed]

MacLeod, D. I., & Boynton, R. M. (1979). Chromaticity diagram showing cone excitation by stimuli of equal luminance. *Journal of the Optical Society of America, 69,* 1183–1186. [PubMed]

Meadows, J. C. (1974). Disturbed perception of colours associated with localized cerebral lesions. *Brain, 97,* 615–632. [PubMed]

Merabet, L. B., Swisher, J. D., McMains, S. A., Halko, M. A., Amedi, A., Pascual-Leone, A., et al. (2007). Combined activation and deactivation of visual cortex during tactile sensory processing. *Journal of Neurophysiology, 97,* 1633–1641. [PubMed] [Article]

Merigan, W., Freeman, A., & Meyers, S. P. (1997). Parallel processing streams in human visual cortex. *Neuroreport, 8,* 3985–3991. [PubMed]

Merigan, W. H. (1996). Basic visual capacities and shape discrimination after lesions of extrastriate area V4 in macaques. *Visual Neuroscience, 13,* 51–60. [PubMed]

Mollon, J., Newcombe, F., Polden, P., & Ratcliff, G. (1980). On the presence of three cone mechanisms in a case of total achromatopsia. In G. Verriest (Ed.), *Colour vision deficiencies* (vol. 5, pp. 130–135). Bristol, UK.

Mullen, K. T., Dumoulin, S. O., McMahon, K. L., de Zubicaray, G. I., & Hess, R. F. (2007). Selectivity of human retinotopic visual cortex to S-cone-opponent, L/M-cone-opponent and achromatic stimulation. *European Journal of Neuroscience, 25,* 491–502. [PubMed]

Murphey, D. K., Yoshor, D., & Beauchamp, M. S. (2008). Perception matches selectivity in the human anterior color center. *Current Biology, 18,* 216–220. [PubMed]

Nathans, J. (1989). The genes for color vision. *Scientific American, 260,* 42–49. [PubMed]

Neitz, J., & Jacobs, G. H. (1990). Polymorphism in normal human color vision and its mechanism. *Vision Research, 30,* 621–636. [PubMed]

Noll, D. C., Cohen, J. D., Meyer, C. H., & Schneider, W. (1995). Spiral K-space MR imaging of cortical activation. *Journal of Magnetic Resonance Imaging, 5,* 49–56. [PubMed]

Pasupathy, A., & Connor, C. E. (2002). Population coding of shape in area V4. *Nature Neuroscience, 5,* 1332–1338. [PubMed]

Press, W. A., Brewer, A. A., Dougherty, R. F., Wade, A. R., & Wandell, B. A. (2001). Visual areas and spatial summation in human visual cortex. *Vision Research, 41,* 1321–1332. [PubMed]

Roorda, A., & Williams, D. R. (1999). The arrangement of the three cone classes in the living human eye. *Nature, 397,* 520–522. [PubMed]

Rüttiger, L., Braun, D. I., Gegenfurtner, K. R., Petersen, D., Schönle, P., & Sharpe, L. T. (1999). Selective color constancy deficits after circumscribed unilateral brain lesions. *Journal of Neuroscience, 19,* 3094–3106. [PubMed] [Article]

Schein, S. J., Marrocco, R. T., & de Monasterio, F. M. (1982). Is there a high concentration of color-selective cells in area V4 of monkey visual cortex? *Journal of Neurophysiology, 47,* 193–213. [PubMed]

Schnapf, J. L., Kraft, T. W., Nunn, B. J., & Baylor, D. A. (1988). Spectral sensitivity of primate photoreceptors. *Visual Neuroscience, 1,* 255–261. [PubMed]

Seidemann, E., Poirson, A. B., Wandell, B. A., & Newsome, W. T. (1999). Color signals in area MT of the macaque monkey. *Neuron, 24,* 911–917. [PubMed] [Article]

Sereno, M. I., Dale, A. M., Reppas, J. B., Kwong, K. K., Belliveau, J. W., Brady, T. J., et al. (1995). Borders of multiple visual areas in humans revealed by functional magnetic resonance imaging. *Science, 268,* 889–893. [PubMed]

Solomon, S. G., & Lennie, P. (2005). Chromatic gain controls in visual cortical neurons. *Journal of Neuroscience, 25,* 4779–4792. [PubMed] [Article]

Solomon, S. G., & Lennie, P. (2007). The machinery of colour vision. *Nature Reviews, Neuroscience, 8,* 276–286. [PubMed]

Solomon, S. G., Peirce, J. W., & Lennie, P. (2004). The impact of suppressive surrounds on chromatic properties of cortical neurons. *Journal of Neuroscience, 24,* 148–160. [PubMed] [Article]

Solomon, S. G., White, A. J., & Martin, P. R. (2002). Extraclassical receptive field properties of parvocellular, magnocellular, and koniocellular cells in the primate lateral geniculate nucleus. *Journal of Neuroscience, 22,* 338–349. [PubMed] [Article]

Stepniewska, I., & Kaas, J. H. (1996). Topographic patterns of V2 cortical connections in macaque monkeys. *Journal of Comparative Neurology, 371,* 129–152. [PubMed]

Stockman, A., MacLeod, D. I., & Johnson, N. E. (1993). Spectral sensitivities of the human cones. *Journal of the Optical Society of America A, Optics, Image Science, and Vision, 10,* 2491–2521. [PubMed]

Takechi, H., Onoe, H., Shizuno, H., Yoshikawa, E., Sadato, N., Tsukada, H., et al. (1997). Mapping of cortical areas involved in color vision in non-human primates. *Neuroscience Letters, 230,* 17–20. [PubMed]

Tjan, B. S., Lestou, V., & Kourtzi, Z. (2006). Uncertainty and invariance in the human visual cortex. *Journal of Neurophysiology, 96,* 1556–1568. [PubMed] [Article]

Tootell, R. B., & Hadjikhani, N. (2001). Where is 'dorsal V4' in human visual cortex? Retinotopic, topographic and functional evidence. *Cerebral Cortex, 11,* 298–311. [PubMed] [Article]

Tootell, R. B., Nelissen, K., Vanduffel, W., & Orban, G. A. (2004). Search for color 'center(s)' in macaque visual cortex. *Cerebral Cortex, 14,* 353–363. [PubMed] [Article]

Van Essen, D. C., Lewis, J. W., Drury, H. A., Hadjikhani, N., Tootell, R. B., Bakircioglu, M., et al. (2001). Mapping visual cortex in monkeys and humans using surface-based atlases. *Vision Research, 41,* 1359–1378. [PubMed]

Van Essen, D. C., Newsome, W. T., & Maunsell, J. H. (1984). The visual field representation in striate cortex of the macaque monkey: Asymmetries, anisotropies, and individual variability. *Vision Research, 24,* 429–448. [PubMed]

Wade, A. R., Brewer, A. A., Rieger, J. W., & Wandell, B. A. (2002). Functional measurements of human ventral occipital cortex: Retinotopy and colour. *Philosophical Transactions of the Royal Society of London B: Biological Sciences, 357,* 963–973. [PubMed] [Article]

Walsh, V., Butler, S. R., Carden, D., & Kulikowski, J. J. (1992). The effects of V4 lesions on the visual abilities of macaques: Shape discrimination. *Behavioural Brain Research, 50,* 115–126. [PubMed]

Walsh, V., Carden, D., Butler, S. R., & Kulikowski, J. J. (1993). The effects of V4 lesions on the visual abilities of macaques: Hue discrimination and colour constancy. *Behavioural Brain Research, 53,* 51–62. [PubMed]

Walsh, V., Kulikowski, J. J., Butler, S. R., & Carden, D. (1992). The effects of lesions of area V4 on the visual abilities of macaques: Colour categorization. *Behavioural Brain Research, 52,* 81–89. [PubMed]

Wandell, B. A. (1995). *Foundations of vision*. Sunderland, MA.

Wandell, B. A. (1999). Computational neuroimaging of human visual cortex. *Annual Review of Neuroscience, 22,* 145–173. [PubMed]

Wandell, B. A., Dumoulin, S. O., & Brewer, A. A. (2006). Computational neuroimaging: Color signals in the visual pathways. *Neuro-ophthalmology, 23,* 324–343.

Wandell, B. A., Dumoulin, S. O., & Brewer, A. A. (2007). Visual field maps in human cortex. *Neuron, 56,* 366–383. [PubMed]

Williams, D., Sekiguchi, N., & Brainard, D. (1993). Color, contrast sensitivity, and the cone mosaic. *Proceedings of the National Academy of Sciences of the United States of America, 90,* 9770–9777. [PubMed] [Article]

Williams, D. R., & Coletta, N. J. (1987). Cone spacing and the visual resolution limit. *Journal of the Optical*

Society of America A, Optics and Image Science, 4, 1514–1523. [PubMed]

Xiao, Y., Wang, Y., & Felleman, D. J. (2003). A spatially organized representation of colour in macaque cortical area V2. *Nature, 421,* 535–539. [PubMed]

Zeki, S. (1983). Colour coding in the cerebral cortex: The responses of wavelength-selective and colour-coded cells in monkey visual cortex to changes in wavelength composition. *Neuroscience, 9,* 767–781. [PubMed]

Zeki, S. (1990a). A century of cerebral achromatopsia. *Brain, 113,* 1721–1777. [PubMed]

Zeki, S. (1990b). Parallelism and functional specialization in human visual cortex. *Cold Spring Harbor Symposia on Quantitative Biology, 55,* 651–661. [PubMed]

Zeki, S. (1993). *A vision of the brain*. London: Blackwell Scientific Publications.

Zeki, S. (1996). Are areas TEO and PIT of monkey visual cortex wholly distinct from the fourth visual complex (V4 complex)? *Proceedings of the Royal Society B: Biological Sciences, 263,* 1539–1544. [PubMed]

Zeki, S. (2003). Improbable areas in the visual brain. *Trends in Neurosciences, 26,* 23–26. [PubMed]

Zeki, S., & Bartels, A. (1999). The clinical and functional measurement of cortical (in)activity in the visual brain, with special reference to the two subdivisions (V4 and V4 alpha) of the human colour centre. *Philosophical Transactions of the Royal Society of London B: Biological Sciences, 354,* 1371–1382. [PubMed] [Article]

Zeki, S., Watson, J. D., Lueck, C. J., Friston, K. J., Kennard, C., & Frackowiak, R. S. (1991). A direct demonstration of functional specialization in human visual cortex. *Journal of Neuroscience, 11,* 641–649. [PubMed] [Article]

Zeki, S. M. (1971). Cortical projections from two prestriate areas in the monkey. *Brain Research, 34,* 19–35. [PubMed]

Zeki, S. M. (1973). Colour coding in rhesus monkey prestriate cortex. *Brain Research, 53,* 422–427. [PubMed]